DESIGN METHODOLOGY FOR A SELF-OSCILLATING RESONANT CONVERTER BASED ON NORMALIZED ANALYSIS APPLIED TO A LOW POWER TOPOLOGY

Thiago C. Naidon
Departamento de Processamento de Energia Elétrica
Universidade Federal de Santa Maria
Santa Maria, Brasil
thiagonaidon@utfpr.edu.br

Lucas S. Mendonça
Departamento de Processamento de Energia Elétrica
Universidade Federal de Santa Maria
Santa Maria, Brasil
lucassangoi1993@gmail.com

Rafael F. Raposo
Departamento de Processamento de Energia Elétrica
Universidade Tecnológica Federal do Paraná
Apucarana, Brasil
rafaelfernandes.raposo@gmail.com

André M. Nicolini
Departamento de Processamento de Energia Elétrica
Universidade Federal de Santa Maria
Santa Maria, Brasil
andrenicoliniee@gmail.com

Fábio E. Bisogno
Departamento de Processamento de Energia Elétrica
Universidade Federal de Santa Maria
Santa Maria, Brasil
fbisogno@gepoc.ufsm.br

***Abstract*—This work presents a design methodology for resonant converters with self-oscillating switching with focus on low power and voltage applications. For this, the concepts of parameter normalization are used, in which it is possible to design the converter independent of the circuit variables, considering only the resonant characteristics such as quality factor, normalized angular frequency, among others. Applications involving low power systems, ranging from tens to hundreds of *miliWatts*, with energy conversion from alternative sources, also known as Energy Harvesting (EH) systems, have been the focus of several studies involving resonant converters. The use of such converters is favorably viewed due to the reduction of switching losses as well as higher power density because the used topology operates in a self-oscillating manner. The simulation and experimental results are presented to validate such theoretical analysis.**

***Index Terms*—Self-Oscillating DC-DC Converter, Low Voltage and Power Circuit, Resonant Converters, Normalized Analysis, Soft Switching.**

I. Introduction

The need for external power devices (batteries) is directly linked to the load. It's possible, for example, an EH (Energy Harvesting) based system tu use only a capacitor as power storage element. [1].

This study was financed in part by the Coordenação de Aperfeiçoamento de Pessoal de Nível Superior - Brasil (CAPES/PROEX) - Finance Code 001. The authors would like to thank the national council for scientific and technological development (CNPq) for all financial, technical and scientific support.

The quick evolution of microelectronic industry and CMOS (Complementary Metal Oxide Semiconductor) process technology has reduced the circuits power consume allowing the use of auto-powered power systems. [3].

The common battery-based power source has important maintenance, discard and lifetime limitations, being the latter quite reduced, making undesired for some application, like wireless sensors nodes.

There is a need to implement new power strategies for such autonomous sensors, increase technology awareness and absorption, eliminating battery replacement as an important operational and environmental issue. [15].

As evidenced, the battery has limited charge, in other words, there is a limited power quantity drain from the battery to the electronic circuit [4]. The autonomy of a circuit depend, therefore, of his power drain, as well battery power storage capability. Besides that, the battery occupies a significant area of the electronic device, as an example, a sensor node. Battery-powered sensors, if exposed to unfavorable conditions, such high temperature, chemical environment, and others, have their use unfeasible. [6].

The need to use a battery, on the other hand, is a common solution when the EH system cannot provide enough power for the continuum run of the application. In this case, the EH system can periodically recharge the battery, condition that increases the autonomy of the device but do not prevent the need of a battery replacement over time. This situation exacerbates the solid waste scenario, making its management a major global challenge and a bottleneck for the electronic device development industry of primary battery-powered. [9].

Many physical processes occur around nodes, whose energy can be captured and used to power wireless sensors [16]: sun brightness, moonlight, vibration, low potential heat, electromagnetic radiation at different frequencies, thermal energy using thermoelectric generators.

This paper proposes a project methodology for a self-oscillating resonant converter for low voltage and power. It is used a normalization of paramters technique allowing the system to be designed from abacus, independently of real system parameters. The system becomes dependent only of the normalized parameters, such as: normalized resonant frequency, and the inverse of the transfer power ratio. The document is organized as follows: Section II presents the converter and principles of operation, in III brings the modeling through circuit variables, in the IV the normalized analysis is presented for the converter under study and, in V presents the project considering specifications for an EH application. The results are presented in section VI and finally in section VII the conclusions are presented.

II. Self-oscillating Resonant Converter Based on Meissner Oscillator

The proposed converter operates with low voltage levels and power, being indicated for applications such as sensors nodes, or other applications involving such features. In order to exemplify the application was used a sensor node that requires a power drain of $3mW$ to $15mW$.

Low power converters require especial attention and specific projects [14]. The main features to be analysed is the efficiency and starter voltage levels of the converter.

There are basically two possibilities for starting a low power converter: the first solution is with an external assistant for the start and the other possibility is the use of a circuit for starting at low voltage. Considering the first solution there are three assistant possibilities such as: an external battery, a pre-charged capacitor or a mechanical switch. [6].

The low voltage switched capacitor converters are widely used in applications involving voltages below $1V$ [10]. The architecture for this converter topology is optimized for operation at low voltage.

There are several techniques that are used to reduce the threshold voltage values of the semiconductor switches.The starting voltage can be $300mV$ or lower, however, small voltage values may present stability issues. [13].

The second category involving self-powered converters makes use of DC-DC resonant converters. In this category, the Meissner oscillator use is generally present [11]. The main advantage of using this topology is the low starting voltage value, as well as the capacity of obtaining high voltage values, by using a transformer.

The proposed resonant converter is in the voltage and power levels of the order of tens of *miliWatts* and *miliVols*, where the converters are self-starting and correspond to a low input voltage (starting at $45mV$).

A. Converter Operation

The analyzed converter for this application uses a starting circuit due to low voltage power supply, such circuit is shown in Figure 1 where the main converter and the starting auxiliary circuit are presented. It should be noted that the starting circuit offers small influence with the main converter, and its analysis scorned in this paper.

For the first operation mode the switch J_1 (JFET) is connected in parallel to switch S_1 (NMOS) and allows the autonomous start, due to their ability to conduct with voltage thresholds close to zero. When applying a positive voltage through V_{CC}, the current I_1 circulates through the primary winding induces voltage in the secondary winding of the transformer. From the positive polarization in S_1 and the capacitor C_1 is discharged, so there is current in the intrinsic diode of S_1 and the voltage at C_1 becomes negative. When it reaches a sufficiently high value, the current I_1 makes the trigger voltage of J_1 decreases and, because the conduction resistance is high, the J_1 switch stop the conduction.

In this context, the auxiliary starting circuit operates in to disconnect the load from the oscillator circuit, during initialization of the circuit via S_2 switch. This disconnection is intended to reduce the equivalent capacitance of the secondary and ensure that there is a longer time constant even during the switching of only the J_1 switch.

In the second mode of operation the switch J_1 is turned-off conduction, and the V_{CC2} voltage is sufficiently large to force conduction through the S_1 switch, marking the passage of the transitory state to the stationary state, with high efficiency, since the conduction losses in S_1 are much smaller than in J_1. By means of the increasing voltage in the secondary of the transformer, the Greinacher voltage multiplier, formed by the diodes and capacitors (D_1, D_2, C_3 and C_4), operates as follows: during the stage where the voltage V_{CC2} is negative, current flows through the diode D_1 charging the capacitor C_3 with the C_5 capacitor voltage and, in the moment that V_{CC2} voltage changes polarity, the C_3 capacitor discharges part of its energy through the D_2 diode, charging the C_4 capacitor with the C_3 capacitor voltage, plus the secondary winding voltage V_{CC2}, ensuring a voltage value sufficient to trigger the S_2 switch in order to impose the input in conduction, then the transfer of energy to the load occurs. The D_3 and D_4 diodes are part of the signal rectification circuit allowing the output signal to be DC.

The waveforms for G_{S1} switch signal, V_{out} output, voltage on V_{S1} switch and current I_{S1} on switch are shown in Figure 2.

III. Converter Modeling Through Circuits Variables

Considering a state-space model with the state arrays A_I, A_{II} and input arrays B_I, B_{II}, where subscript "I" means the first mode of operation, when the switch is on and the

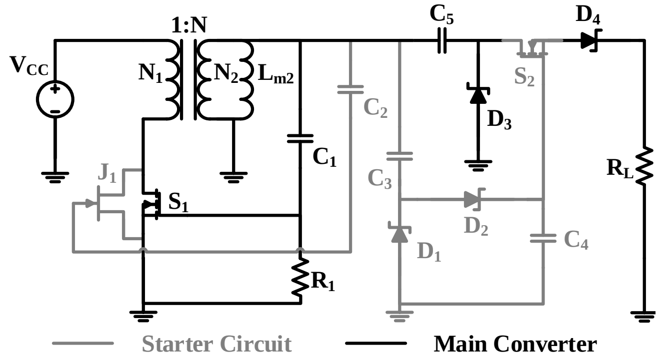

Fig. 1. Self-oscillating resonant converter.

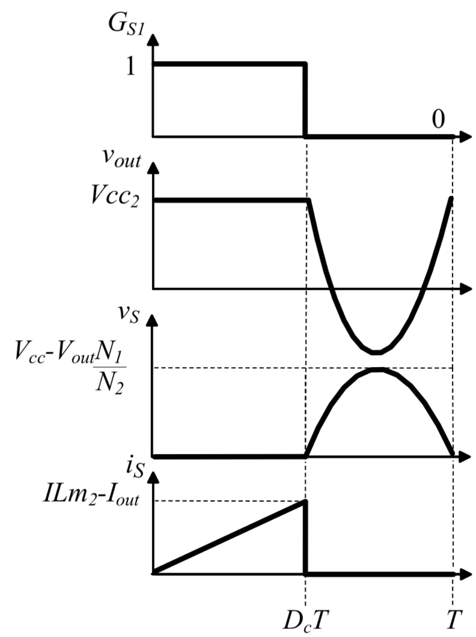

Fig. 2. Waveforms for the gate signal of the switch G_{S1}, output voltage v_{out}, switch voltage v_{S1} and switch current i_{S1} of the resonant converter based on the Meissner oscillator.

subscript "II" is representing the second mode of operation, representing when the switch is off.

For the equation, it is considered V_{in} as the input voltage, V_{out} as the output voltage,V_{Lm2} the voltage at the L_{m2} inductor, V_{C1} the voltage at the C_1 capacitor,V_S the voltage at the S_1 switch, i_{in} the input current, i_{out} the output current, i_{Lm2} the current at the L_{m2} inductor , i_{C1} the current in the C_1 capacitor, i_{S1} the current in S_1 switch,V_{CC2} the voltage in the secondary winding of the connected inductor, N_1 is the number of turns in the primary winding, N_2 the number of turns in the secondary winding and I_{CC2} the current in the secondary winding of the connected inductor. For the proposed converter, consider the vector x as being $x = \{i_{Lm2}, v_{C1}\}$.The system is represented per:

$$\begin{aligned} Mode\ \ I : \dot{\mathbf{X}} &= \tfrac{d[\mathbf{x(t)}]}{dt} = \mathbf{A_I}(\mathbf{x}) + \mathbf{B_I V_{CC2}} \\ Mode1\ \ II : \dot{\mathbf{X}} &= \tfrac{d[\mathbf{x(t)}]}{dt} = \mathbf{A_{II}}(\mathbf{x}) + \mathbf{B_{II} V_{CC2}} \end{aligned} \tag{1}$$

By means of the Kirchhoff's Laws of voltage and Current it is possible to establish the equations below.

$$\mathbf{A_I} = \begin{bmatrix} 0 & 0 \\ 0 & -\frac{1}{C_1 R_1} \end{bmatrix}; \mathbf{B_I} = \begin{bmatrix} \frac{1}{L_{m2}} \\ \frac{1}{C_1 R_1} \end{bmatrix} \tag{2}$$

$$\mathbf{A_{II}} = \begin{bmatrix} -\frac{R_1 R_L}{L_{m2}(R_1+R_L)} & \frac{R_L}{L_{m2}(R_1+R_L)} \\ -\frac{R_L}{C_1(R_1+R_L)} & -\frac{1}{C_1(R_1+R_L)} \end{bmatrix}; \mathbf{B_{II}} = \begin{bmatrix} 0 \\ 0 \end{bmatrix} \tag{3}$$

Defining the output variables of interest in a output vector,the representation is given by:

$$\begin{aligned} y(t) = & \frac{i_{Lm_2}}{I_{CC2}}, \frac{i_S}{I_{CC2}}, \frac{iC_1}{I_{CC2}}, \frac{i_{out}}{I_{CC2}} \frac{i_{in}}{I_{CC2}}, \\ & \frac{v_{Lm_2}}{V_{CC2}}, \frac{v_S}{V_{CC2}}, \frac{vC_1}{V_{CC2}}, \frac{v_{R1}}{V_{CC2}} \end{aligned} \tag{4}$$

considering the output equations as:

$$\begin{aligned} Mode\ \ I &: \mathbf{y}(t) = \mathbf{C_I x}(t) + \mathbf{D_I V_{CC2}} \\ Mode\ \ II &: \mathbf{y}(t) = \mathbf{C_{II} x}(t) + \mathbf{D_{II} V_{CC2}} \end{aligned} \tag{5}$$

$$\mathbf{C_I} = \begin{bmatrix} \frac{1}{I_{CC2}} & 0 \\ \frac{1}{I_{CC2}} & -\frac{1}{R_L I_{CC2}} \\ 0 & -\frac{1}{R_L I_{CC2}} \\ 0 & 0 \\ \frac{1}{I_{CC2}} & -\frac{1}{R_L I_{CC2}} \\ 0 & 0 \\ 0 & 0 \\ 0 & \frac{1}{V_{CC2}} \\ 0 & -\frac{1}{V_{CC2}} \end{bmatrix}; \mathbf{D_I} = \begin{bmatrix} 0 \\ \left(1 + \frac{R_L}{R_1}\right) \frac{1}{I_{CC2}} \\ \frac{1}{R_1 I_{CC2}} \\ \frac{1}{R_L I_{CC2}} \\ \left(1 + \frac{R_L}{R_1}\right) \frac{1}{I_{CC2}} \\ \frac{1}{V_{CC2}} \\ 0 \\ 0 \\ \frac{1}{V_{CC2}} \end{bmatrix} \tag{6}$$

$$\mathbf{C_{II}} = \begin{bmatrix} \frac{1}{I_{CC2}} & 0 \\ 0 & 0 \\ \left(-\frac{R_L}{R_L+R_1}\right) \frac{1}{I_{CC2}} & \left(-\frac{R_L}{R_L+R_1}\right) \frac{1}{R_L I_{CC2}} \\ \left(\frac{R_L}{R_L+R_1} - 1\right) \frac{1}{I_{CC2}} & \left(\frac{R_L}{R_L+R_1}\right) \frac{1}{R_L I_{CC2}} \\ 0 & 0 \\ \left(\frac{R_1 R_L}{(R_L+R_1)}\right) \frac{1}{I_{CC2}} & \left(\frac{R_L}{R_L+R_1}\right) \frac{1}{I_{CC2}} \\ 0 & \frac{1}{V_{CC2}} \\ 0 & \frac{1}{V_{CC2}} \\ -\left(\frac{R_1 R_L}{(R_L+R_1)}\right) \frac{1}{I_{CC2}} & \left(\frac{R_L}{R_L+R_1}\right) \frac{1}{I_{CC2}} \end{bmatrix}; \mathbf{D_{II}} = \begin{bmatrix} 0 \\ 0 \\ 0 \\ 0 \\ 0 \\ 0 \\ \frac{1}{V_{CC2}} \\ 0 \\ 0 \end{bmatrix} \tag{7}$$

IV. Normalized Analysis for the Resonant Converter

The independent variable t is changed by ωt by means of the following mathematical operation:

$$\frac{d\left[x\left(t\right)\right]}{dt} \overset{\omega}{\Leftrightarrow} \omega \frac{d\left[x\left(\omega t\right)\right]}{d\omega t} \tag{8}$$

With the change of variable in relation to time it is possible to obtain the normalized resonance frequency A_1 relating the operating frequency ω and the angular frequency A_1 through of [10] and [9].

$$A_1 = \frac{\omega_1}{\omega} \tag{9}$$

$$\omega_1 = \frac{1}{\sqrt{L_{m_2} C_1}} \tag{10}$$

The combination of dissipate components with reactive components of a resonant circuit forms the quality factor Q.The number of quality factors present in a circuit is equal to the number of resistors simplified or also known as reduced resistances [12]. For the converter addressed in this study, it is defined a number of two quality factors, which is justified by the number of reduced resistances presented in [11].

$$\begin{aligned} Q_L &= \tfrac{R_L}{L_{m_2}\omega_1} = C_1 \omega_1 R_L \\ Q_1 &= \tfrac{R_1}{L_{m_2}\omega_1} = C_1 \omega_1 R_1 \end{aligned} \tag{11}$$

By using the aforenmentioned relationships, it is possible to converter the state-space matrices into a normalized representation as a function of A_1, Q_1 and Q_L. The normalized state space is presented in: [12].

$$\begin{aligned} Mode\ \ I : \dot{\mathbf{X}} &= \tfrac{d[\mathbf{x}(\omega \mathbf{t})]}{d\omega t} = \mathbf{E_I}(\mathbf{x}) + \mathbf{F_I} \\ Mode\ \ II : \dot{\mathbf{X}} &= \tfrac{d[\mathbf{x}(\omega \mathbf{t})]}{d\omega t} = \mathbf{E_{II}}(\mathbf{x}) + \mathbf{F_{II}} \end{aligned} \tag{12}$$

in which,

$$\mathbf{E_I} = \begin{bmatrix} 0 & 0 \\ 0 & -Q_1 A_1 \end{bmatrix}; \mathbf{F_I} = \begin{bmatrix} 1 \\ Q_1 A_1 \end{bmatrix} \tag{13}$$

$$\mathbf{E_{II}} = \begin{bmatrix} -\frac{A_1}{Q_1 + Q_L} & \frac{Q_1}{Q_1 + Q_L} \\ -\frac{{A_1}^2 Q_1}{Q_1 + Q_L} & -\frac{A_1 Q_1 Q_L}{Q_1 + Q_L} \end{bmatrix}; \mathbf{F_{II}} = \begin{bmatrix} 0 \\ 0 \end{bmatrix} \tag{14}$$

where:

$\mathbf{E_I}$ is the normalized state matrix related to $\mathbf{A_I}$;
$\mathbf{F_I}$ is the normalized input matrix related to $\mathbf{B_I}$;
$\mathbf{E_{II}}$ is the normalized state matrix related to $\mathbf{A_{II}}$;
$\mathbf{F_{II}}$ is the normalized input matrix related to $\mathbf{B_{II}}$;

The inverse transfer power ratio a, is defined as,

$$a = \frac{V_{CC2}}{I_{CC2}} R_L \tag{15}$$

The voltage Vcc_2 will be automatically normalized from the arrays D_I and D_{II}. The output equations for the normalized system are:

$$\begin{aligned} Mode\ \ I : \mathbf{y}(\omega t) &= \mathbf{G_I}\mathbf{x}(\omega t) + \mathbf{H_I} \\ Mode\ \ II : \mathbf{y}(\omega t) &= \mathbf{G_{II}}\mathbf{x}(\omega t) + \mathbf{H_{II}} \end{aligned} \tag{16}$$

Rearranging the terms according to the normalization elements, the results are presented in [17] e [18].

$$\mathbf{G_I} = \begin{bmatrix} a\frac{A_1}{Q_L} & 0 \\ a\frac{A_1}{Q_L} & -a\frac{Q_1}{Q_L} \\ 0 & -a\frac{Q_1}{Q_L} \\ 0 & 0 \\ a\frac{A_1}{Q_L} & -a\frac{Q_1}{Q_L} \\ 0 & 0 \\ 0 & 0 \\ 0 & 1 \\ 0 & -1 \end{bmatrix}; \mathbf{H_I} = \begin{bmatrix} 0 \\ a\left(1 + \frac{Q_1}{Q_L}\right) \\ a\frac{Q_1}{Q_L} \\ a \\ a\left(1 + \frac{Q_1}{Q_L}\right) \\ 1 \\ 0 \\ 0 \\ 1 \end{bmatrix} \tag{17}$$

$$\mathbf{G_{II}} = \begin{bmatrix} a\frac{A_1}{Q_L} & 0 \\ 0 & 0 \\ -\frac{Q_1}{(Q_1+Q_L)} a\frac{A_1}{Q_L} & -a\frac{Q_1}{(Q_1+Q_L)} \\ a\frac{A_1}{Q_L}\left(\frac{Q_1}{(Q_1+Q_L)} - 1\right) & a\frac{Q_1}{(Q_1+Q_L)} \\ 0 & 0 \\ -\frac{A_1}{(Q_1+Q_L)} & \frac{Q_1}{(Q_1+Q_L)} \\ 0 & 1 \\ 0 & 1 \\ -\frac{A_1}{(Q_1+Q_L)} & \frac{Q_1}{(Q_1+Q_L)} \end{bmatrix}; \mathbf{H_{II}} = \begin{bmatrix} 0 \\ 0 \\ 0 \\ 0 \\ 0 \\ 0 \\ 1 \\ 0 \\ 0 \end{bmatrix} \tag{18}$$

where:

$\mathbf{G_I}$ is the normalized output matrix related to $\mathbf{C_I}$;
$\mathbf{H_I}$ is the normalized transmission matrix related to $\mathbf{D_I}$;
$\mathbf{G_{II}}$ is the normalized output matrix related to $\mathbf{C_{II}}$;
$\mathbf{H_{II}}$ is the normalized transmission matrix related to $\mathbf{D_{II}}$;

By defining soft-switching conditions as, initial capacitor C_1 voltage $v_{C1}(0)$ equal to the inverse of the normalized angular frequency, the system operated in ZVS for any operating point. The generative hypothesis of ZVS is that the initial voltage of the capacitor $v_{C1}(0)$, is equal to the inverse of the normalized angular frequency, $\frac{1}{A_1}$. The system of output equations requires a numerical value representing the power transfer ratio to the system, where it is possible to obtain this information without need of parameters, as presented in [10].

The system solution returns the behavior of the output variables for any input.

V. Normalized Design of the Self-Oscillating Resonant Converter

The converter design may involve the design option for one or more elements, however, it was decided to use a commercially coupled inductor. The input voltage V_{CC}, the power output P_{out}, switching frequency f and the duty cycle D_c are defined by the designer. The parameters A_1, Q_1 and Q_L are defined according to the selected operating point.

1) Definition of the duty cycle D_c, frequency f, V_{CC} voltage input voltage and output power P_{out}.
2) Select A_1, Q_1 and Q_L and the transfer power ratio for ZVS condition according to the duty cycle.
3) Calculate the operating frequency f and the voltage at the secondary winding V_{CC2}:

$$\omega = 2\pi f \tag{19}$$

$$Vcc_2 = Vcc\left(\frac{N_2}{N_1}\right) \tag{20}$$

4) Calculate resistors R_L and R_1 and capacitor C_1 by the following equations:

$$R_L = \omega Q_L A_1 L_{m_2} \tag{21}$$

$$R_1 = \omega Q_1 A_1 L_{m_2} \tag{22}$$

$$C_1 = \frac{Q_L}{\omega A_1 R_L} \tag{23}$$

It should be noted that the converter operates at a duty cycle of 50%, however, the project predicts that the variation can be realized also characterizing a converter with controllable duty cycle.

The design parameters obtained through simulation in mathematical software are presented in Table I.

VI. Results

The theoretical, simulation and experimental results are going to be presented. Theoretical results were obtained in the software Mathematica 10 and simulations by using the LTspice VII software. Table I shows the converter parameters:

TABLE I
DESIGN PARAMETERS

Parameters	Value	Parameters	Value
Lm_2	75 mH	C_1	1 nF
fs	10 kHz	A_1	1,82944
V_{CC}	50 mV	D	0,5
P_{out}	10 mV	R_L	470 kΩ
Q_1	1,6	Q_L	0,016

Table II presents a comparison among some DC-DC type converters with shared similar characteristics of low voltage and power.

The converter of the present study stood out in two relevant factors, the starting voltage and also the output voltage, however, left something to be desired in terms of efficiency, however, the results for a discrete implementation were satisfactory.

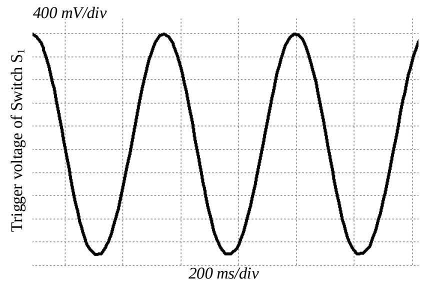

Fig. 3. Simulation result for switch S_1 voltage.

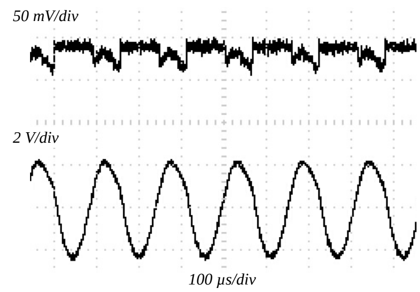

Fig. 4. Experimental results for switch S_1 voltage.

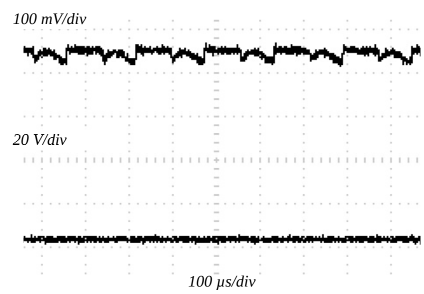

Fig. 5. Experimental results for input and output voltage, respectively.

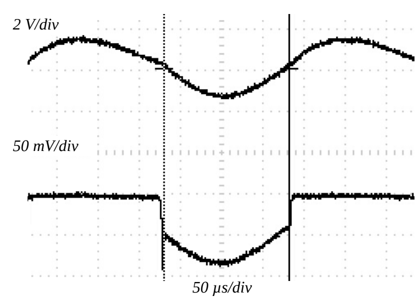

Fig. 6. Experimental results for switch S_1 voltage.

TABLE II
COMPARISON AMONG DC-DC CONVERTERS FOR LOW VOLTAGE AND POWER APPLICATIONS

Parameter	RICHELLI (2012)	LUO (2018)	ADAMI (2013)	Present Study
Prototyping	Mixed	Integrado	Discrete	Discrete
Minimum input voltage	120 mV	210 mV	200 mV	50 mV
Output Voltage	1,2 V	1,1 V	2,5 V	3,7 V
Efficiency	30%	71%	25%	12,50%

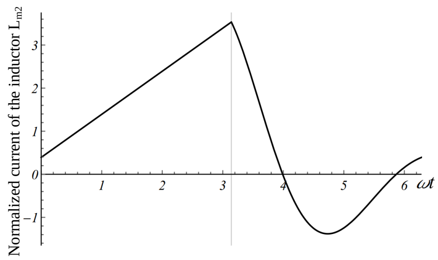

Fig. 7. Theoretical results for inductor L_{m_2} current.

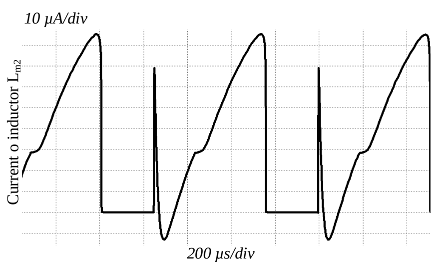

Fig. 8. Simulation results for inductor L_{m_2} current.

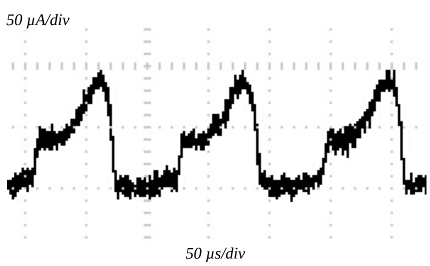

Fig. 9. Experimental results for inductor L_{m_2} current.

VII. Conclusion

An design methodology based on normalized analysis was developed for a self-oscillating resonant converter, whose application was used for low voltage and power. The auxiliary starting circuit had the analysis disregarded by noting that it is not part of the circuit of steady state operation. One of the main objectives of the design methodology was the independence of circuit parameters and specifications, such as, frequency, input and output voltage, power, among others. Another purpose was that the circuit had its operation in the ZVS region, minimizing switching losses, increasing the efficiency of the converter, which is interesting considering that the circuit is designed for low power levels. The auxiliary starting circuit based on a voltage multiplier of the Greinacher type, played its role successfully. In addition to being a low cost circuit, being formed only by capacitors and diodes, its principle of operation is simple, not interfering directly in the operation of the main converter. The proposed work presented theoretical and simulation results in the software LTspice VII and Mathematica 10, which are in agreement with the waveforms obtained by experimental means, which confirms the hypothesis of this research.

References

[1] M. R. Mhetre, N. S. Nagdeo, H. K. Abhyankar, "Micro energy harvesting for biomedical applications: A review", pp. 1–5, apr 2011.

[2] V. Raghunathan, A. Kansal, J. Hsu, J. Friedman, M. Srivastava, "Design considerations for solar energy harvesting wireless embedded systems", in IPSN 2005. Fourth International Symposium on Information Processing in Sensor Networks, 2005., pp. 457–462, IEEE, 2005.

[3] Y. K. Ramadass, A. P. Chandrakasan, "A batteryless thermoelectric energy-harvesting interface circuit with 35mV startup voltage", in 2010 IEEE International Solid-State Circuits Conference - (ISSCC), pp. 486–487, IEEE, feb 2010.

[4] L. Xie, R. Du, "Harvest human kinetic energy to power portable electronics", Journal of Mechanical Science and Technology, vol. 26, no. 7, pp. 2005–2008, jul 2012.

[5] S. Moon, J.-S. Lai, B. Park, J. Lee, D. Koo, "Design and control of battery charger for portable human powered generator", in 2014 IEEE Applied Power Electronics Conference and Exposition - APEC 2014, pp. 1590–1597, IEEE, mar 2014.

[6] S.-E. Adami, N. Degrenne, C. Vollaire, B. Allard, F. Costa, "Ultra-low power, low voltage, autonomous resonant DC-DC converter for low power applications", in 4th International Conference on Power Engineering, Energy and Electrical Drives, pp. 1222–1228, IEEE, may 2013.

[7] S. Roundy, P. K. Wright, J. M. Rabaey, Energy Scavenging for Wireless Sensor Networks, Springer US, Boston, MA, 2004.

[8] J. Painuly, "Barriers to renewable energy penetration; a framework for analysis", Renewable Energy, vol. 24, no. 1, pp. 73–89, sep 2001.

[9] W. N. Mbav, S. Chowdhury, "A comparative study of two different stand-alone schemes based on Landfill Gas Energy projects", in 2013 48th International Universities' Power Engineering Conference (UPEC), pp. 1–5, IEEE, sep 2013.

[10] L. Mendonça, T. Naidon, F. Bisogno, M. Martins, "Equivalence Transformation And Normalized Analysis For Design A Resonant Converter For Energy Harvesting Applications", Eletrônica de Potência, vol. 22, no. 4, pp. 372–379, dec 2017.

[11] SEIKO INSTRUMENTS, Ultra-Low Voltage Operation Charge Pump IC For Step-Up DC-DC Converter Startup: S-882Z Series, 2015, rev. 1.2.

[12] "A Sub-10 mV Power Converter With Fully Integrated Self-Start, MPPT, and ZCS Control for Thermoelectric Energy Harvesting", IEEE Transactions on Circuits and Systems I: Regular Papers, vol. 65, no. 5, pp. 1744–1757, may 2018.

[13] M. Pollak, L. Mateu, P. Spies, "STEP-UP DC-DCCONVERTER WITH COUPLED INDUCTORS FOR LOW INPUT VOLTAGES", pp. 1–7, 2008.

[14] C.-T. Chen, Linear System Theory and Design, 3rd ed., Oxford University Press, Inc., New York, NY, USA, 1998.

[15] X. Yue, M. Kauer, M. Bellanger, O. Beard, M. Brownlow, D. Gibson, C. Clark, C. MacGregor, and S. Song, "Development of an indoor photovoltaic energy harvesting module for autonomous sensors in building air quality applications," IEEE Internet of Things Journal, vol. 4, no. 6, pp. 2092–2103, Dec 2017.

[16] S. Chalasani, and J. M. Conrad, "A Survey o f Energy Harvesting Sources for Embedded Systems," IEEE SoutheastCon, Huntsville, AL, 2008, pp. 442-447.